Journal of Applied Phycology (2025) 37:837–853
https://doi.org/10.1007/s10811-025-03455-7

RESEARCH

Phycosphere of an algal co-culture phycoremediation system: Stability of bacterial communities in an *Oedogonium-Stigeoclonium* co-culture during cultivation in microbially rich wastewater

Ethan Wood[1,2] · **Bente Edvardsen**[2] · **Kari Skjånes**[3] · **Luka Šupraha**[1]

Received: 20 November 2024 / Revised: 16 January 2025 / Accepted: 17 January 2025 / Published online: 7 February 2025
© The Author(s) 2025

Abstract

Algal-based wastewater remediation systems (phycoremediation) include phycosphere bacterial communities that influence algal growth, pollutant remediation, and downstream applications of biomass as fertilizers or bio-stimulants. This study investigated the bacterial community dynamics in a novel phycoremediation system using a co-culture of the green algae *Stigeoclonium* sp. and *Oedogonium vaucheri*. Bacterial abundance was estimated using flow cytometry (FCM), while community composition was assessed through 16S rRNA gene metabarcoding. Additionally, 28 bacterial strains were isolated from the bioremediation experiment, cultured, genetically characterized for identification and screened for production of the auxin phytohormone indole-3-acetic acid (IAA). Metabarcoding showed that the free-living bacterial community consisted of bacteria from both the wastewater effluent and the algal inocula, while the attached phycosphere community was dominated by bacteria from the algal inocula, indicating the stability of the algae-associated phycosphere. Taxa known to include plant growth-promoting bacteria (PGPB) were abundant, and several strains produced IAA. The bacterial community composition, combined with the potential production of phytohormone by isolated bacteria indicates symbiotic or commensal algae-microbe interactions within the phycosphere bacterial communities. Sterile filtration of wastewater effluent, including only the algal inoculum bacterial communities, reduced algal biomass production and increased bacterial abundance. This study highlights the critical role of microbial interactions in engineered ecosystems and provides insights for optimizing algal-based wastewater treatment technologies.

Keywords Phycoremediation · Phycosphere · Wastewater · Phytohormones · Filamentous algae

Introduction

The phycosphere is a region around an alga where interaction and chemical exchange occur between a community of associated bacteria and the host alga (Seymour et al. 2017; Burgunter-Delamare et al. 2024). Generally, there is an expected commensal or mutualistic relationship between an algal host and its phycosphere bacteria (Seymour et al. 2017; Baker et al. 2022). Bacteria can take advantage of algal exudates, and algae can benefit from bacterial metabolites and the remineralization of limiting nutrients. Additionally, photoautotrophic algae and heterotrophic bacteria may benefit each other through the production and consumption of CO_2 and O_2 (Seymour et al. 2017; Fu et al. 2020). In cases where interactions are antagonistic, bacteria can compete with algae for limiting nutrients or produce algacidal compounds compromising algal growth or causing cell lysis (Seymour et al. 2017; Burgunter-Delamare et al. 2024).

Similar to how the microbiology of the rhizome and the characterization of plant growth-promoting bacteria (PGPB) has been applied in agricultural sciences, an enhanced understanding of the phycosphere has the potential to enable methodological developments in algal biotechnology (Kim et al. 2014; Seymour et al. 2017; Kimbrel et al. 2019; Durán et al. 2022). The community composition and stability of the phycosphere can promote algal growth, enhance

✉ Ethan Wood
ethan.wood@niva.no

1 Norwegian Institute for Water Research (NIVA), Økernveien 94, 0579 Oslo, Norway

2 Department of Bioscience, University of Oslo (UIO), Blindernveien 31, 0371 Oslo, Norway

3 Norwegian Institute of Bioeconomy Research (NIBIO), Høgskoleveien 7, 1433 Ås, Norway

nutrient uptake, and impart resistance to stress (Kim et al. 2014; Fulbright et al. 2018; Liu et al. 2020a). Similar taxa of bacteria are associated with algal cultures and with plant rhizospheres, including PGPB (Ramanan et al. 2015). Typical PGPB traits are nitrogen fixation, phosphate solubilization, and phytohormone production including that of phytohormone indole-3-acetic acid (IAA) (De-Bashan et al. 2008; Glick 2012; Ramanan et al. 2015; Etesami and Glick 2024). These traits may have similar relevance within the phycosphere and it has been demonstrated that PGPB isolated from the rhizosphere of plants can assemble in the phycosphere and promote algal growth (Durán et al. 2022). This parallel between the rhizosphere and PGPB, and the phycosphere and algal growth promoting bacteria has led to the new terminology, using "microalgal growth promoting bacteria" (MGPB) when referring specifically to algae–bacteria interactions (Palacios et al. 2022).

During phycoremediation, i.e., the remediation of wastewater by algae cultivation, wastewater replaces clean water and commercial fertilizers while simultaneously algae enhance the remediation of nutrients and pollutants thus reducing anthropogenic eutrophication (Renuka et al. 2015; Priyadharshini et al. 2021). Wastewaters are microbially diverse and phycoremediation systems harbor complex ecologies with various phycosphere-host interactions influencing algal productivity and pollutant remediation (Renuka et al. 2015; Ashraf et al. 2023; Blifernez-Klassen et al. 2023). During phycoremediation, bacteria are contributed by multiple sources. Wastewater and the algal inoculum have their own distinct communities, and contamination from the environment is unavoidable. The bacterial communities of algal inoculum may include MGPB (Kimbrel et al. 2019) and the stability of the phycosphere when challenged by microbially rich wastewater may influence algal growth and the remediation potential of the of the system.

In this study a mesocosm experiment was conducted to simulate the phycoremediation process and investigate the bacterial community composition of the phycosphere, as well as the influence of the wastewater microbiome on algal growth and nutrient depletion. This experiment involved a co-culture of filamentous green algae implemented to further remediate tertiary municipal wastewater effluent. Metabarcoding (eDNA) targeting amplification of the 16S rRNA gene was employed to describe the composition and diversity of bacterial communities and to evaluate the relative contribution of bacteria from the algal inoculum and wastewater to the attached phycosphere and free-living communities. An isolation effort was successful in establishing single strain bacterial cultures and linking them to highly abundant amplicon sequence variants (ASVs) in the metabarcode data. The isolated bacterial strains were then screened for production of IAA indicating a role in phycosphere bacteria – algae interactions.

Materials and methods

Algal strains

Filamentous chlorophyte algae were chosen for their presumed resistance to grazers and suitability for low-cost mechanical harvesting (Liu et al. 2020b). A co-culture of *Stigeoclonium* sp. (K-0018) and *Oedogonium vaucheri* (K-0094) was selected based on growth in wastewater effluent at relevant temperatures and ease of scaled-up cultivation in commercial medium. Strain K-0018 was isolated from a freshwater pond in Avernakø, Denmark in 1992 and strain K-0094 from ditch in Amager, Denmark in 1954. These strains are maintained as non-axenic mono-algal cultures at the Norwegian Culture Collection of Algae (NORCCA) at 15 °C in Z8 medium with soil extract and additional vitamins (Watanabe 2005). Prior to experiments the culture medium was changed to commercially available Cell-Hi HP (0.5 g L^{-1}, Varicon Aqua Solutions, UK). To remove unattached bacterial cohabitants the algal strains were cleaned by capillary re-isolation. Individual short filaments were washed with sterile medium using a glass Pasteur pipette and inoculated into well-plates with medium. Cultures were allowed to recover and were maintained in 25 mL sterile cell culture flasks before scaling up as 2 L mono-algal inoculum cultures in mesocosms under experimental conditions.

Wastewater effluent and treatments

Municipal wastewater effluent collected in March from the VEAS AS treatment plant in Slemmestad, Norway, was used in the experiments. Having undergone conventional physical, chemical, and biological treatments, the tertiary effluent meets discharge regulations for nutrient pollutants, however approximately 30 % of the initial inorganic nitrogen along with other pollutants still remain, potentially contributing to anthropogenic eutrophication in the Oslofjord (Källqvist et al. 2002; Vestfjorden Wastewater Company 2023). This study aims to evaluate the potential of phycoremediation to further reduce residual nitrogen. Before use, the effluent was vacuum filtered through Whatman 6.0 µm mesh size, 90 mm, grade 3 qualitative filter paper (Cytiva, USA) to remove larger particles and organisms.

The experimental design consisted of three treatments with four replicates each. The Filtered Treatment (FT) involved adding 300 mL of each of the two algal monocultures to eight liters of the 6.0 µm filtered wastewater effluent and distributing two liters of this into four mesocosm containers. The aim of the FT treatment was to determine if the phycosphere community maintains community

structure in microbially diverse wastewater effluent. The Sterile Treatment (ST) followed the same inoculation procedure as the FT treatment but with effluent vacuum prefiltered through 0.22 µm mesh size, 90 mm hydrophilic polycarbonate membranes (Merck, Germany). Exclusion of the wastewater effluent microbiome in the ST treatment provided a control for the investigation of the impact of the effluent microbiome on algal growth and bacterial community composition. The ST treatment is not sterile as it includes non-axenic algal inocula. The third treatment, Control Treatment (CT), consisted of the 6.0 µm filtered effluent without algal inoculation and provided a control for the effect of algal inoculation on nutrient remediation and the bacterial community.

Mesocosm design

Mesocosms were designed to emulate the physical conditions of a proposed raceway pond system at the VEAS wastewater treatment plant. Closed mesocosms were constructed from acrylic cylinders with an internal diameter of 15.3 cm and height of 20.7 cm. Mixing was provided by constant air bubbling supplied through a 20 mL pipette fixed through a hole in the mesocosm lid. To maintain inorganic carbon availability and prevent pH elevation, CO_2 was automatically sparged through the airline when pH reached 8.9. The culture room maintained a temperature between 12 and 16 °C, reflecting the range experienced at the VEAS plant. Illumination was provided by full-spectrum LED 16 hours per day, at a mean intensity of 450 µmol photons m^{-2} s^{-1} measured with a light meter (model MQ-510, Apogee Instruments, USA) directly above the bioreactor lid.

Algal growth and nutrient depletion

The growth of algal biomass was measured as a daily increase in cell dry weight (cdw). Mesocosms were gently swirled to resuspend any sedimented biomass and 40 mL was sampled though the pipette used to sparge air and CO_2. Samples were vacuum filtered on pre-weighed Whatman GF/C glass fiber filters, 47 mm before drying and weighing using a moisture analyzer scale (model MB 64, VWR, USA. Filters were heated to 120 °C and weighed continuously until stable within 0.001 g for 20 seconds.

Filtrates from cell dry weight measurements were frozen and stored for analysis of inorganic macronutrients necessary for algal growth. Analysis was performed using colorimetric assay kits (Hach Lange, USA): Orthophosphate (LCK 349), Nitrate + Nitrite (LCK 339), and Ammonium (LCK 304) (Van Den Hendeb 2015).

Bacterial abundance

Bacterial abundance was estimated by flow cytometry (FCM) and by plate counts of colony-forming units (CFU). Samples for FCM were taken on days 0, 4, and 9 while plate counts were conducted on days 0 and 9.

For FCM, samples were preserved in EM grade glutaraldehyde with 1% final concentration, (Sigma-Aldrich, USA) and stored at 4 °C. Samples were diluted 1:100 in PBS buffer and staining was performed for 10 min at room temperature with SYBR Green I (Sigma_Aldrich, USA) diluted 1:100 in Tris buffer. Samples (10 µL) were run on a NovoCyte Advanteon flow cytometer (Agilent Technologies, USA) using a blue excitation laser (488 nm) and detectors for green (533/30 nm) and red (> 670 nm) fluorescence. Bacteria were separated from background noise using electronic gating following the approach described by Prest et al. (2013). This resulted in a mean of 5403 events per 10 µL sample determined to be bacteria cells by gating.

Plate count samples for CFU were stored overnight at 4 °C, diluted in a six-step 10-fold series, and 100 µL was plated on R2A medium agar plates (Reasoner and Geldreich 1985). Plates were incubated for 5 days at 22 °C and colonies were counted ensuring an approximate 10-fold difference between plates in the series.

DNA extraction for 16S metabarcoding

Samples (20 mL) were collected for DNA extraction at both the start and end of the experiment in duplicates. At the start, samples were taken from the wastewater effluent and the two algal inoculum cultures as well as the algal stock cultures from which the inoculum was scaled up. At the end of the experiment, after the nine-day incubation period, all 12 mesocosms were sampled. To capture the attached phycosphere-enriched communities, samples were first filtered through 5.0 µm hydrophilic polycarbonate membranes (47 mm, Isopore, MilliporeSigma, USA) using vacuum filtration to collect algal biomass. The filtrate was then passed through 0.2 µm hydrophilic polycarbonate membranes (47 mm, Isopore, MilliporeSigma, USA) to capture free-living communities. Filters were stored at −80°C until extraction.

For improved DNA extraction, filters were cut into small pieces using sterile equipment. DNA extraction was performed with the NucleoSpin Soil kit (Macherey-Nagel, Germany) following the manufacturer's protocol and using the provided lysis buffer L-1. DNA concentration was measured using the Qubit HS assay (ThermoFisher, USA). Samples with concentrations below 0.1 ng μL^{-1} were excluded from library preparation, while those with higher concentrations were diluted to 5 ng μL^{-1}.

Metabarcoding library preparation and sequencing

To investigate the taxonomic composition and structure of bacterial communities the V3 and V4 regions of the 16S ribosomal RNA gene was selectively amplified by polymerase chain reaction (PCR). Amplification involved the following primers: 341F (Forward - 5'CCTACG GGNGGCWGCAG) and 805NR (Reverse - 5'GACTAC HVGGGTATCTAATCC) (Illumina 2013) modified to include Illumina Nextera index adapters (Illumina, US.). The initial amplification of target DNA was conducted in triplicate 20 µL reactions: 2 µL template, 0.5 µL forward and reverse primers, and 0.2 µL Q5 high fidelity polymerase (Thermo Fisher Scientific, USA). The thermocycler schedule for amplification was 98 °C for 3 min, followed by 20 cycles of 98 °C for 30 s, 48 °C for 30 s, 72 °C for 30 s, then a final extension at 72 °C for 3 min to ensure complete amplification. The product was cleaned using AMpure magnetic beads (Beckman Coulter, USA) according to manufacturer's protocol. Sample specific Nextera indexes (Illumina, USA) were attached to the cleaned and pooled product by a second PCR, 98 °C for 3 s, followed by 15 cycles of 98 °C for 10 s, 66°C for 30 s, 72 °C for 30 s, then a final extension at 72°C for 2 min. Illumina (Miseq V3) 300bp pair-end sequencing was conducted at the Norwegian Sequencing Centre (NSC) at University of Oslo. Sequencing resulted in a mean of 101657 reads per sample.

Bioinformatics

Taxonomic assignment

Mean reads per sample was reduced from 101657 to 63959 by processing. Primer sequences were removed using Cutadapt (v4.1) in Python (v3.1) and remaining bioinformatic analysis was conducted in R (v4.3.1) (Martin 2011). After visually inspecting the sequencing quality, a truncation length of 250 bp was set for forward reads and 200 bp for reverse reads. This was done to maintain a sequencing quality score above 30 and to ensure sufficient overlap for read merging. R package Dada2 (v1.28.0) was employed to remove low-quality reads, merge paired ends, remove chimeric sequences, and assign taxonomy using the Silva database (v138.1) (Callahan et al. 2016). Contaminants were identified and removed using the R package decontam (v1.20.0) prevalence method (Davis et al. 2018). Replicate samples were visualized using the R package phyloseq (v1.44.0) before dereplicating with the function 'merge_samples2', R package speedyseq (v0.5.3.9018) (McMurdie and Holmes 2013; McLaren 2020). Metabarcoding sequences have been submitted to NCBI Sequence Read Archive (SRA) under BioProject PRJNA1190337.

Diversity analysis

Diversity analysis of bacterial communities at the end of the experiment was performed with R packages breakaway (v4.8.4) and DivNet (v0.4.0). R package breakaway estimates richness and standard errors from non-rarified high-diversity count data while accounting for co-occurrence networks (Willis and Bunge 2015). DivNet estimates alpha and beta diversity indices and then implements modeling across predictor variables with function 'betta' from R package beta (Willis and Martin 2022). Richness along with alpha diversity estimates, Shannon index, and Simpson index were compared by linear regression across bacterial communities: CT, FT attached, FT free-living, ST attached, and ST free-living. To evaluate the similarity between communities, we estimated Bray-Curtis dissimilarity with R package DivNet (v0.4.0) and performed non-metric multidimensional scaling (NMDS) analysis to visualize the dissimilarities as an ordination plot, utilizing R package *vegan* (v2.6-4).

ASV tracing to sources

ASVs were traced to a source in either one of the two algal inoculum cultures or the wastewater effluent. This was done to assess the relative contribution of these sources to the mesocosm bacterial communities. An ASV was deemed present in a sample if its count exceeded 0.1 % the maximum observed count for that ASV across the dataset. And a source of an ASV was determined by presence in at least two decontaminated samples from that source and no other source. This approach prevented issues with potential cross-contamination of highly abundant ASVs while preserving the detection of low abundance ASVs. For ASVs traced to a source in either of the algal inoculum cultures (*Stigeoclonium* or *Oedogonium*), it was further indicated if they were present in the original stock culture or only the scaled-up inoculum.

Differential abundance

To investigate differences between the attached phycosphere community and the free-living community in the FT treatment at the ASV level, differential abundance analysis was conducted in R package ALDEx2 (v1.32.0). ALDEx2 models counts using 128 Monte Carlo instances derived from a Dirichlet distribution to estimate differential abundance and provides significance testing as Benjamini-Hochberg corrected p-values obtained from a Wilcoxon test (Gloor 2015). This analysis was performed on unfiltered and unrarefied

data as described in the benchmark study by Nearing et al. (2022).

Bacteria isolation and phylogenetic analysis

Bacterial strains were isolated from culture plates used for enumeration (See "Bacterial abundance") based on colony morphology to obtain both diverse and abundant strains. Individual colonies were selected and inoculated to 50 mL Lennox LB Broth (SigmaAldrich, US.) in 200 mL autoclaved glass culture flasks. Cultures were then plated on R2A agar to confirm single colony morphology. All isolates were maintained on R2A agar, incubated at 25°C until colonies developed, and then stored at 4 °C.

Taxonomic identification of isolated bacteria was performed by barcoding the 16S rRNA gene. Template DNA for PCR was prepared by heating 1.5 mL bacterial culture at 98 °C for 10 min, followed by centrifugation at 11999 × g for 5 min. The supernatant was diluted in Milli-Q water to 10 % concentration before freezing and used directly as PCR template. PCR amplification of the 16S rRNA gene was carried out using primers 27F and 1492R (Abellan-Schneyder et al. 2021) (Eurofins Genomics, Germany), with the following thermocycler program: initial denaturation at 95 °C for 3 min, followed by 30 cycles of 95 °C for 30 s, 56 °C for 30 s, and 72 °C for 1 min, with a final extension at 72 °C for 5 min. The PCR reaction mix consisted of 5 µL of template DNA, 1 µL of each primer, and GoTaq Green Master Mix (ThermoFisher, US.). PCR products were assessed by agarose gel electrophoresis and purified using ExoSap-IT enzymatic degradation (ThermoFisher, US.). Sanger sequencing was performed using three sequencing primers: 27F, 515F, and 1492R (Abellan-Schneyder et al. 2021) (Eurofins Genomics, Germany). Sequences were aligned using online software Benchling editor before BLAST query to NCBI (Benchling Biology Software 2004). The best match 16S rRNA gene sequence was downloaded from GenBank as reference sequences for taxonomic assignment. Consensus sequences for each bacterial strain isolate have been submitted to the National Center for Biotechnology Information (NCBI) GenBank database with accession numbers (Table S2).

A phylogenetic tree was constructed to refine the taxonomic assignment of the isolated strains and to establish correspondence with metabarcoding ASVs. Sanger sequences from the 28 isolated bacterial strains along with their reference sequences (See "Metabarcoding library preparation and sequencing") were aligned using MAFFT (v.7). ASVs from the metabarcoding results were then incorporated into the alignment using MAFFT's 'add fragments' function.

From the 2491 ASVs, 308 were added to the phylogenetic alignment to establish correspondence to the isolated bacteria Sanger sequences. Selection of ASVs was based on both family and genus assignment. All ASVs with genus level assignment matching the reference sequences were included along with the most abundant ASVs from each genus within the corresponding family.

A Maximum Likelihood tree was inferred in R package phangorn (v.2.11.1). Function 'modelTest' was implemented to select the nucleotide substitution model TIM2+G(4)+I based on minimizing AIC and BIC scores (Schliep 2019). Standard bootstrapping was performed for 500 iterations. The tree was rooted using *Mycobacterium tuberculosis* as an outgroup, chosen for its distant phylogenetic relationship to the isolated strains. The taxonomy of the isolated bacterial strains was refined and correspondence to ASVs was established by shared tree nodes.

Auxin screening

Selected bacterial isolates representing unique 16S rRNA gene sequences were screened for potential production of the phytohormone auxin IAA by the Salkowski reagent method. A positive test result is indicated by the oxidation of auxins resulting in a pink color measurable by spectrophotometry. Cultures were grown in triplicates at room temperature on a rotary shaker in Lenox LB broth (ThermoFisher, USA), supplemented with 0.15 g L^{-1} L-tryptophan (VWR, USA), until visibly dense. Tryptophan is a precursor in the biosynthesis of IAA. Samples (1.5 mL) were centrifuged at 11999 × g for 5 min (model 5804 R, Eppendorf, USA), and 700 µL of the supernatant was mixed with an equal volume of Salkowski reagent (0.5 M $FeCl_3$ in 35% $HClO_4$, 1:50 v/v) (Gang et al. 2019). The mixture was incubated in the dark for 30 min, and absorbance was measured at 536 nm using a spectrophotometer against a negative control (media + reagent).

To compare concentrations across bacterial strains and normalized by cell density (turbidity), we used a linear model with log (A_{536}/A_{600}) as response and strain as predictor. Predictions of this model can be interpreted as the logarithm of IAA absorbance (560 nm) at unit turbidity (A_{600} = 1) for each strain. Multiplying the inverse log-transformed predictions with the IAA calibration factor gives strain-specific estimates for the IAA concentration in cultures at the reference turbidity (A_{600} = 1). Estimates were converted to mg L^{-1} IAA using a standard curve established with a 7-step, 2-fold dilution series ranging from 3.13 to 100 mg L^{-1} IAA standard (SigmaAldrich, USA).

Results

Algal growth and nutrient depletion

Algal biomass, measured as cell dry weight (cdw) in g L^{-1}, continued to increase until the experiment ended

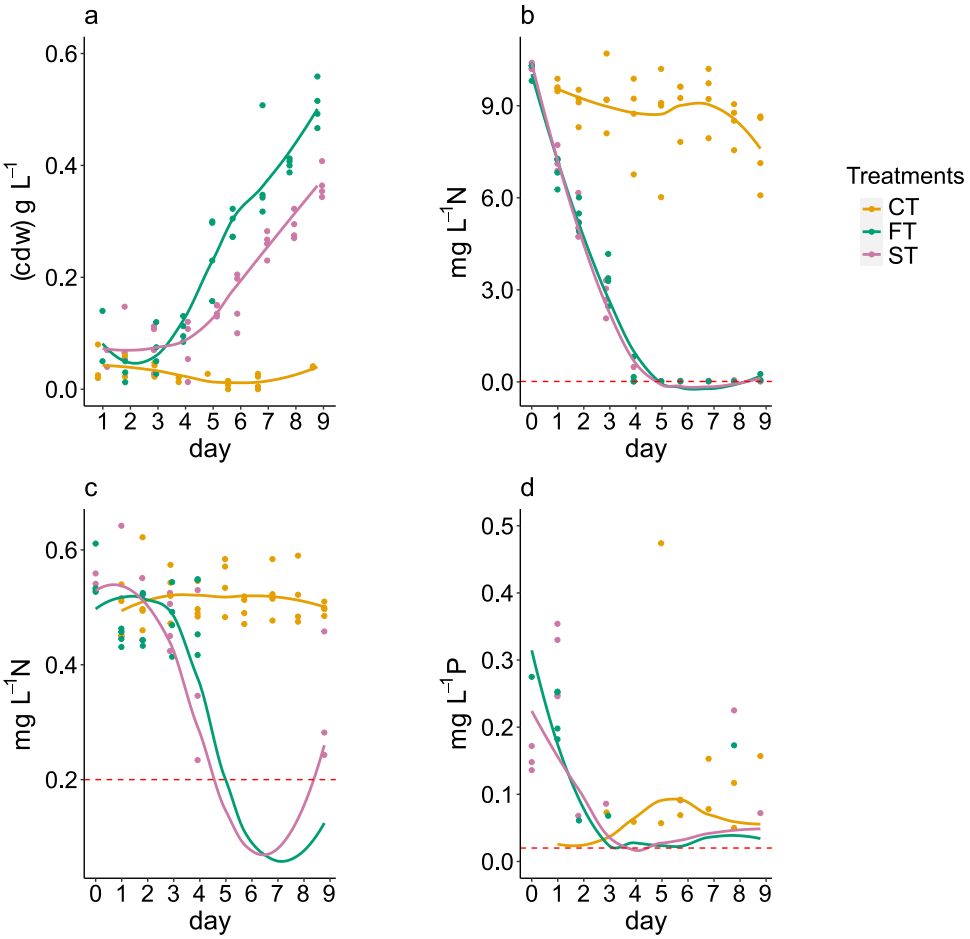


Fig. 1 Biomass growth and nutrient depletion. Treatments: effluent without algal inoculation (CT), 6 µm filtered effluent with algal inoculation (FT), 0.2 µm filtered effluent with algal inoculation (ST). (**a**) Cell dry weight (cdw) measured over the course of the experiment. (**b**) ammonium concentration (**c**) nitrate + nitrite concentration, (**d**) orthophosphate concentration. For (b, c and d) the lower limit of detection for the assay is indicated with a red dashed line. Trend lines show smoothed changes over time using the LOESS algorithm from the ggplot2 package in R

on day nine. From day five onward, cdw was greater in the FT treatment, where the wastewater microbiome was retained, compared to the ST treatment, where the wastewater microbiome was removed. This suggests that the removal of the wastewater microbiome through sterile filtration of the effluent negatively impacted algal productivity (Fig. 1a).

In the ST and FT treatments, with the algal inoculation, ammonium and nitrate were similarly depleted. Whereas, in the CT treatment, with no algal inoculation inorganic nitrogen are not depleted (Fig. 1b and c). Ammonium, the primary source of inorganic nitrogen, was depleted to near detection limits by day four. Nitrate depletion was delayed, but occurred rapidly once ammonium was depleted. In the CT treatment the orthophosphate remained below or near the lower limit of detection 0.02 mg L^{-1} during the course of the experiment suggesting low availability to support algal growth. In the FT and ST treatments, orthophosphate initially measured around 0.2 mg P L^{-1} and was then rapidly depleted (Fig. 1 d). This initially higher concentration was likely a consequence of carryover of residual nutrients with the algal inoculum.

Bacterial abundance

Bacterial abundance estimated by flow cytometry (FCM) increased in the ST treatment during the experiment (Fig. 2 a). Bacterial abundance in the ST treatment had already increased by day four and continued to rise with greater abundance on day nine. This trend was not observed in the FT or CT treatments. Bacterial abundance estimated by plate culture counts on day nine aligned with the FCM results (Fig. 2 b).

Bacterial community composition

Each of the experimental source communities, the two algal inocula and the wastewater effluent, had distinct bacterial communities. Samples were taken in duplicates, and where both samples generated sequencing results, both replicates are displayed to demonstrate the consistency of the method (Fig. 3). The bacterial community was described in the algal inocula as well as the stock culture from which the inocula was scaled up. This revealed shifts in community composition during inoculum cultivation. The inoculum cultures

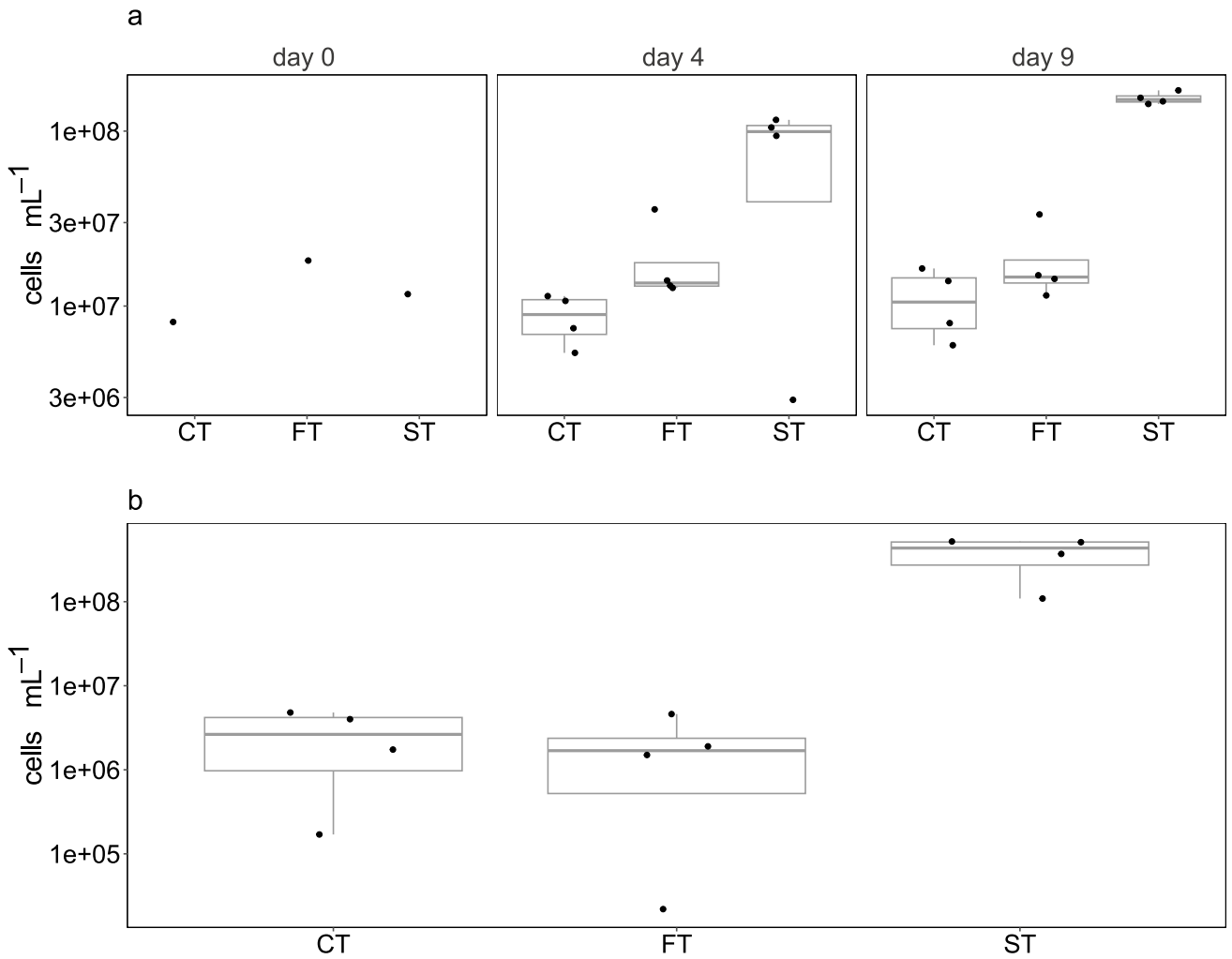


Fig. 2 Mesocosm bacterial abundance. Treatments: effluent without algal inoculation (CT), 6 µm filtered effluent with algal inoculation (FT), 0.2 µm filtered effluent with algal inoculation (ST). (**a**) Bacterial abundance estimated by flow cytometry (FCM) on days 0, 4, and 9 for each treatment. On day 0, a single point represents a sample taken before the inoculated culture was distributed to replicate mesocosms, points on days 4 and 9 show replicate mesocosms. (**b**) Bacterial abundance on day 9 estimated by colony-forming units (CFU) on solid agar. Box plots show the interquartile range

were sampled to differentiate the attached and free-living fractions, while the effluent and the algal stock cultures were only sampled on the 0.2 µm pore size filters and thus revealed the entire bacterial community together.

From the stock culture to the inoculum that was scaled up under experimental conditions the *Stigeoclonium* bacterial community increased in dominance of Flavobacteriales and Burkholderiales with the loss of Pseudomonadales. While the *Oedogonium* bacterial community went from being completely dominated by Rhizobiales in the stock culture to a mix of Rhizobiales and *Sphingomonas* in the inoculum.

The bacterial community in the effluent was predominantly characterized by members of Burkholderiales. Although Burkholderiales was abundant in both the *Stigeoclonium* sp. mono-algal culture and the effluent, the genus-level composition differed between these communities, with *Stigeoclonium* sp. dominated by *Acidovorax* and the effluent dominated by *Polaromonas*.

In the mesocosms at the end of the phytoremediation process, the bacterial communities consisted of a mixture of those from experimental source materials (Fig. 4). The ST treatment contained microbiomes from both mono-algal inocula, while the FT treatment additionally included the effluent microbiome. Differences in community composition were observed between treatments and between attached and free-living communities within treatments.

In the ST treatment, the free-living fraction was dominated by the genus *Limnobacter*. While in comparison the ST attached fraction exhibited a more even taxonomic distribution. In the FT treatment the attached fraction was dominated by bacteria also observed in the algal inocula and ST treatment. The FT free-living fraction showed in addition to

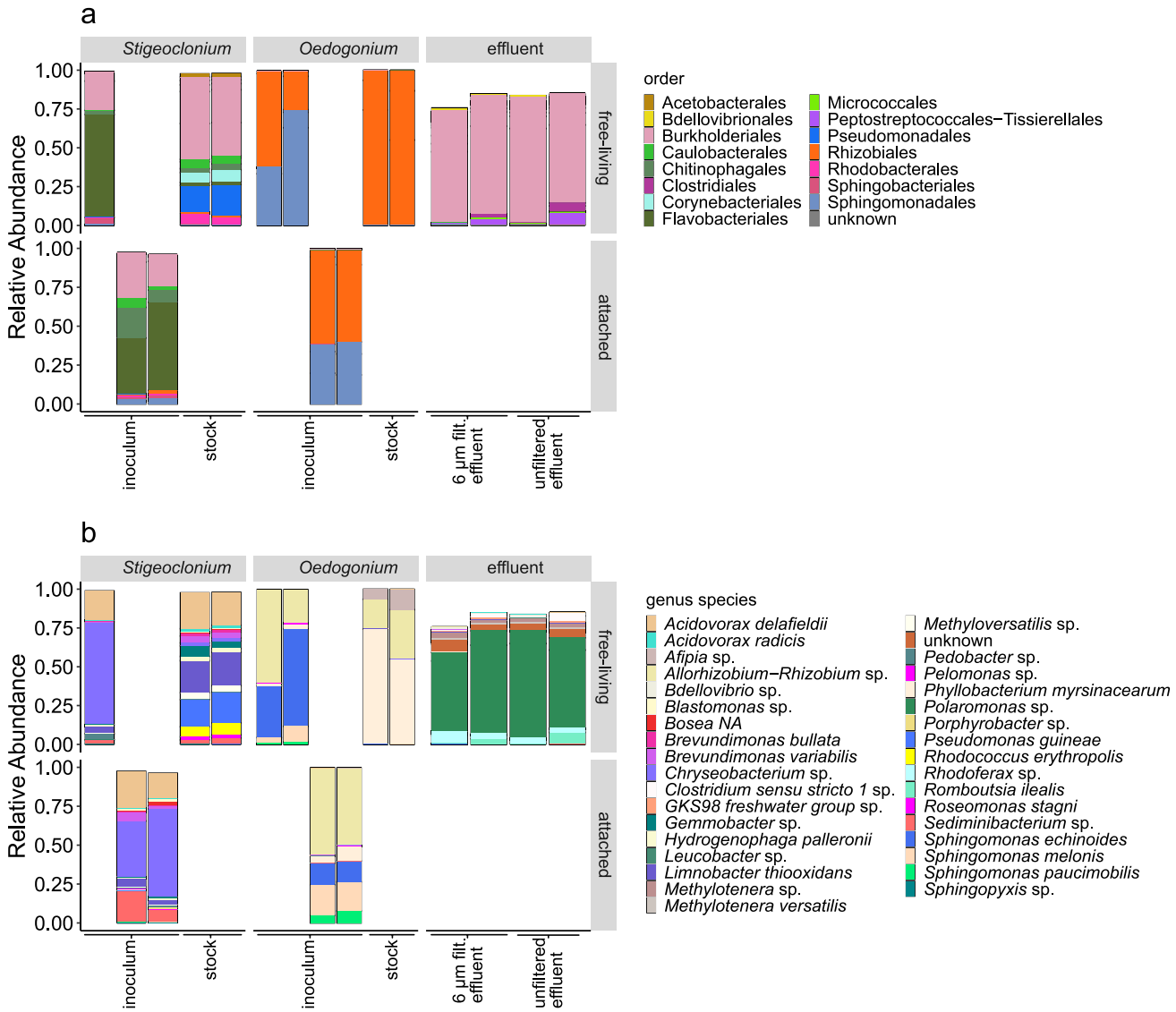


Fig. 3 Composition of source bacterial communities in attached and free-living fractions. Plot displays technical replicate samples. ASVs modeling was performed with R package Dada2 and taxonomic assignment by reference to the Silva database (v138.1). Panels (a) and (b) display the top 50 most abundant ASVs, with (**a**) showing the order level and (**b**) presenting the genus level taxonomic composition

those bacteria observed in the attached fraction several taxa associated with sewage or human gut microbiomes including orders Peptostreptococcales and Clostridiales (Fig. 4). The CT mesocosm communities displayed high variability, but included several dominant orders also found in other treatments, such as Flavobacteriales, Burkholderiales, and Sphingomonadales (Fig. 4, a).

Bacterial diversity

The wastewater effluent was the primary contributor to bacterial diversity in the experiment. Richness was an order of magnitude higher in the FT treatment compared to the ST treatment and was similar in the attached and the free-living communities within each treatment (Fig. 5 a). This result aligns with expectations, as the ST treatment only contained the bacterial communities of the algal inocula.

Simpson's and Shannon alpha diversity indices reflected differences in community structure (Fig. 5 b and c). Within the ST treatment, the attached community had a lower Simpson's index and a greater Shannon index than the free-living community, despite having similar richness indicating that the ST free community had lower evenness. For the CT treatment, the diversity indices showed high variance indicating divergence between the replicate mesocosms in the absence of inoculated alga.

To determine similarity between the bacterial communities across treatments and between the attached and

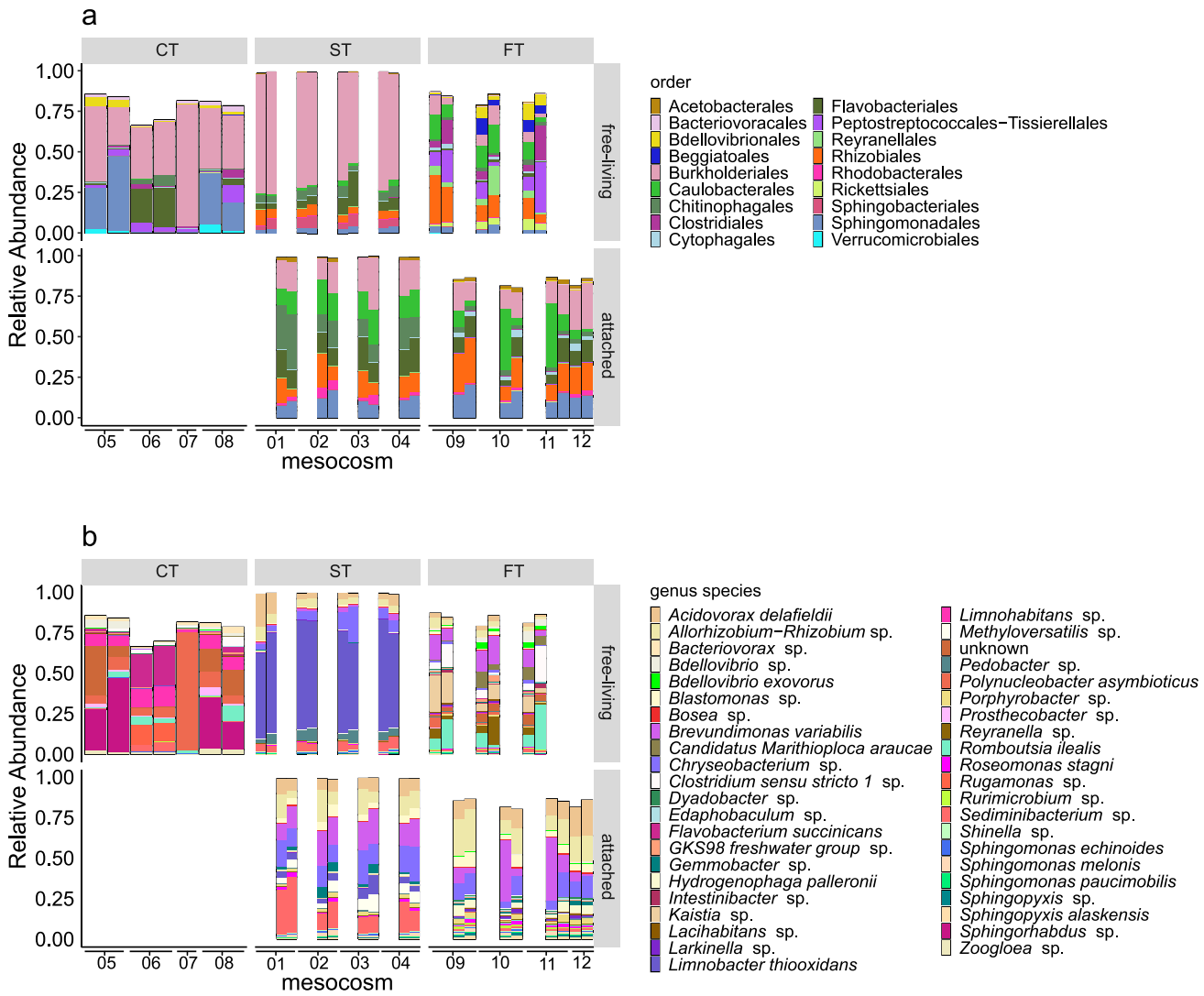


Fig. 4 Composition of bacterial communities in attached and free-living fractions of the mesocosms at the end of the experiment. Plot displays technical replicate samples. ASVs modeling was performed with R package Dada2 and taxonomic assignment by refence to the Silva database (v138.1). Panels (a) and (b) display the top 50 most abundant ASVs, with (**a**) showing the order level and (**b**) presenting the genus level. Mesocosms are divided into treatments: effluent without algal inoculation (CT), 6 µm filtered effluent with algal inoculation (FT), 0.2 µm filtered effluent with algal inoculation (ST)

free-living fractions, NMDS scaling, and ordination of Bray-Curtis dissimilarity was performed (Fig. 6). Greater similarity was observed between the attached fractions across the FT and ST treatments than between the attached and free-living fractions within treatments. The FT attached community was more dissimilar to the effluent than the FT free-living community suggesting the free-living fraction shares community structure with both the effluent and the attached phycosphere fraction. The CT treatment exhibited greater variance between replicate mesocosms than treatments with cultured algae. The introduction of algal co-culture corresponded with lower variance within treatments for both the attached and free-living fractions of the FT treatment.

Tracing ASV to sources

The tracing of ASVs to experimental sources followed an approach based on both prevalence and abundance aimed at assigning a source to the highly abundant ASVs while accounting for cross contamination (See "ASV tracing to sources"). Of the 43 ASVs observed in the *Stigeoclonium* inoculum culture 34 were successfully traced to *Stigeoclonium* as a source, based presence in at least 2 unmerged samples from the *Stigeoclonium* inoculum or stock. In the *Oedogonium* inoculum, 29 ASVs were observed and 14 were traced to the *Oedogonium* as a source. Of the 908 ASVs observed in effluent samples 438 ASVs were traced to the

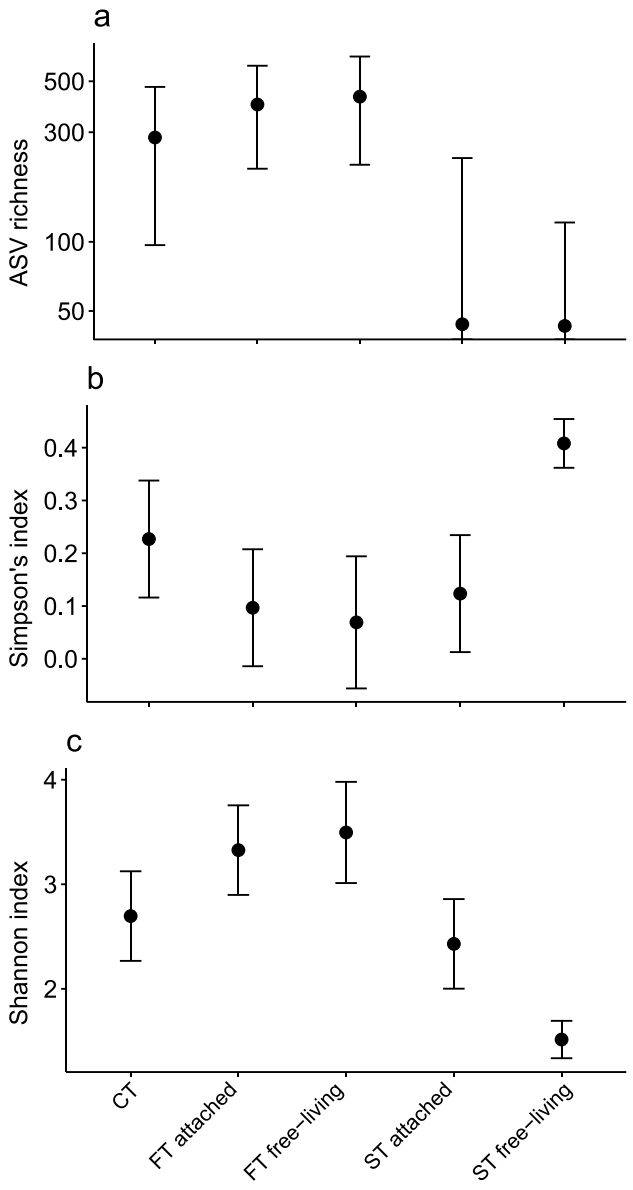


Fig. 5 Alpha diversity index estimates of mesocosm communities at the end of the experiment. (**a**) Richness estimated using the R package Breakaway. (**b**) Simpson's index and (**c**) Shannon index estimated using the R package DivNet. Error bars show 1.96 ×*SE* as the approximate 95 % CI. Communities are indicated by both fraction (free-living and attached) and treatment. Treatments: effluent without algal inoculation (CT), 6 µm filtered effluent with algal inoculation (FT), 0.2 µm filtered effluent with algal inoculation (ST)

effluent as a source. There were 2005 ASVs for which a source was unidentified. The high number of unidentified ASVs likely reflects a mix of low-abundance ASVs or data sparsity, as well as environmental contamination. Most of these unidentified reads were observed predominantly in the CT treatment (Fig. 7 a).

The relative contribution of bacteria from the original biological sources to the mesocosms varied between treatments and size fractions (Fig. 7 a). The bacterial communities of the mono-algal cultures contributed a mean ± range of 81.84 ± 2.87% of reads to the FT-attached fraction, compared to 44.61 ± 12.31% to the free-living fraction (Fig. 7 b). This indicated that bacteria originating from the mono-algal cultures maintained a physical association with the algal biomass when the co-culture was cultivated in microbially rich effluent. The contribution of ASVs by source varied between treatments and community types (Fig. 7 b). In both the ST and FT treatments the *Stigeoclonium* inoculum contributed more reads than the *Oedogonium* inoculum (Fig. 7 a).

Differential relative abundance

Differential relative abundance was estimated to explore differences in community composition at the ASV level between attached and free-living fractions in the FT treatment. Several highly abundant ASVs, with greater abundance in the attached fraction as indicated by a negative effect estimate, had Benjamini-Hochberg corrected p-values (we.eBH) near or below the traditional 0.05 alpha value (Table 1). The most abundant of these, asv0005 and asv0002, both were traced to the *Stigeoclonium* inoculum and were successfully isolated in culture (See "Taxonomic assignment of bacteria isolates"). The only ASV from the *Oedogonium* inoculum that was significantly more abundant in the attached community was asv0010, identified as *S. melonis*. That several ASVs traced to the effluent were more abundant in the attached fraction indicates that there was a degree of colonization of the phycosphere by the wastewater microbiome, however these ASVs tended to be of lower abundance. The complete differential abundance results, including ASVs with corrected p-values greater than 0.1 and ASVs with positive effect estimates indicating greater abundance in the free-living fraction, is provided in the supplemental material (Table S2). ASVs, significantly more abundant in the free-living community, were generally traced to the effluent or they remained unknown source (Table S2).

Taxonomic assignment of bacteria isolates

Phylogenetic analysis of the 28 isolated bacterial strains identified 16 unique 16S rRNA gene Sanger sequences, or phylotypes (Table S2). Reference sequences were obtained by BLAST query of the NCBI GenBank nucleotide database. Taxonomic assignment was further refined by sequence alignment and the inference of a Maximum Likelihood phylogenetic tree. Metabarcode ASV sequences were included in the sequence alignment, and correspondence to isolated bacterial strains was established through a shared terminal node (Fig. S1). To illustrate the phylogeny of the isolated

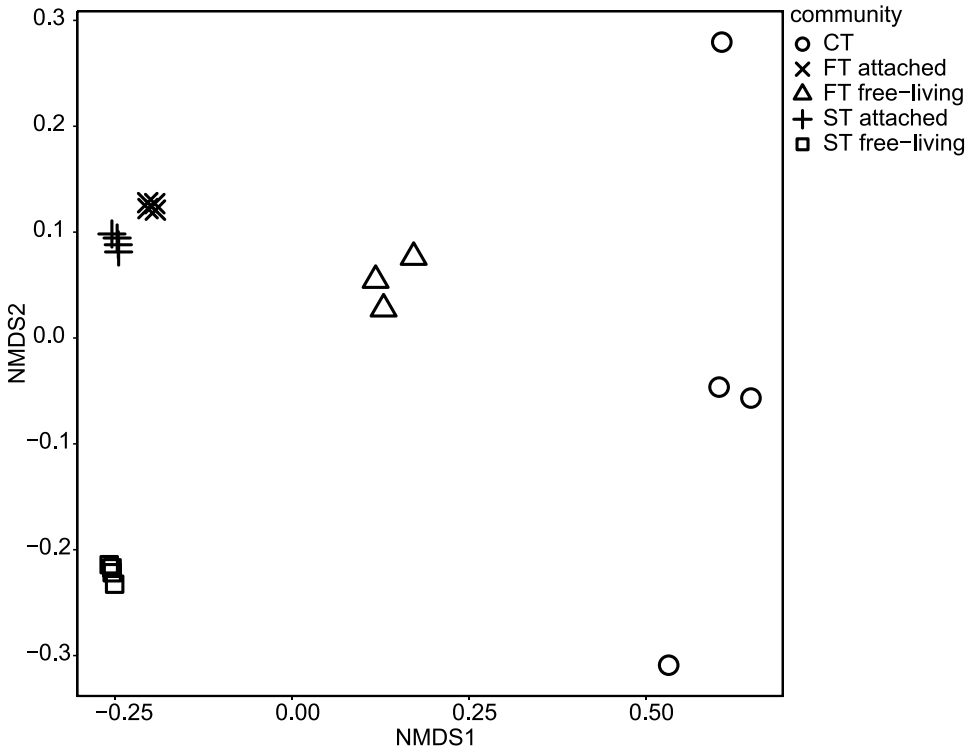


Fig. 6 NMDS ordination of beta diversity estimates, of bacterial communities at the end of the experiment. Bray-Curtis dissimilarity index was estimated by R-package DivNet (v0.4.0) and non-metric multidimensional scaling (NMDS) analysis was performed (stress = 0.0471) using R package *vegan* (v2.6-4). Communities are indicated by both fraction (free-living and attached) and treatment. Treatments: effluent without algal inoculation (CT), 6 µm filtered effluent with algal inoculation (FT), 0.2 µm filtered effluent with algal inoculation (ST)

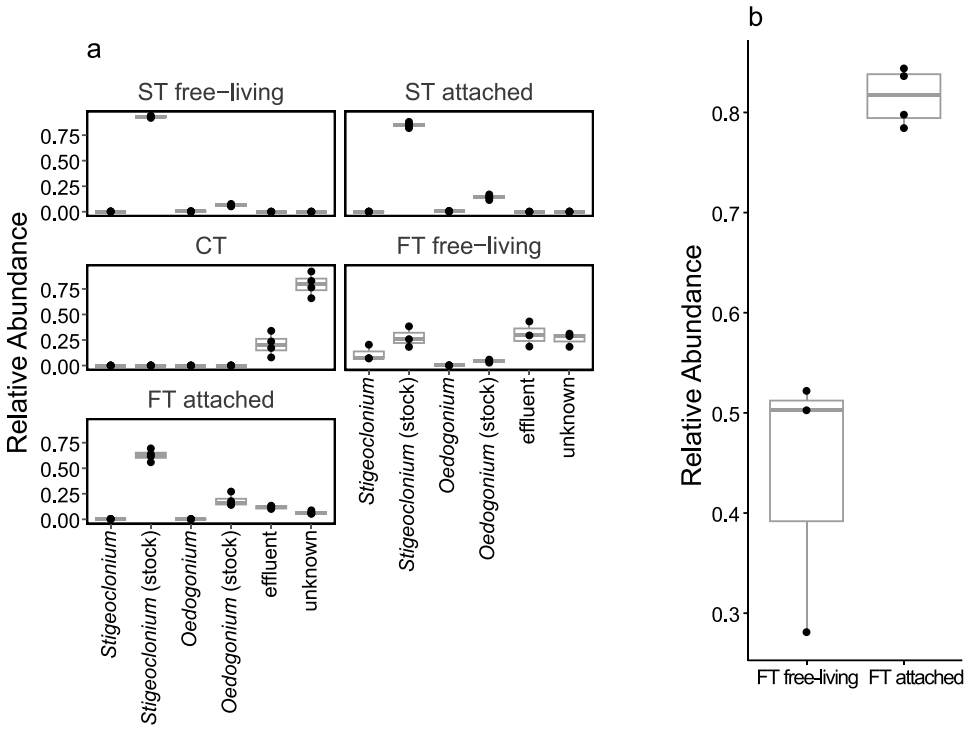


Fig. 7 Relative contribution of sources to mesocosm bacterial communities. (**a**) Contribution of reads from each experimental source to mesocosm communities at the end of the experiment (day 9). (**b**) Contribution of reads from the combined algal inocula *Stigeoclonium* and *Oedogonium* to the FT attached and free-living communities at the end of the experiment. For all plots boxplots show the interquartile range. Communities are indicated by both fraction (free-living and attached) and treatment. Treatments: effluent without algal inoculation (CT), 6 µm filtered effluent with algal inoculation (FT), 0.2 µm filtered effluent with algal inoculation (ST)

bacterial strains alongside their corresponding ASVs, the phylogenetic tree was pruned to include only a single representative phylotype for each isolated strain and its closely related ASVs (Fig. 8). Generally, each isolated phylotype shares a leaf with a single ASV, supporting the idea that each isolate corresponds to a specific ASV. Isolated strain CT-7-1 was the only phylotype that did not align with any ASVs from the metabarcoding results. The bacterial isolates included Bacteriodota, Betaproteobacteria, and Alphaproteobacteria within Pseudomonadota, resulting in three

Table 1 Differential relative abundance between attached and free-living fractions in the FT treatment. Differential abundance was modeled using the R package ALDEx2. A negative effect size indicates enrichment in the attached fraction. Benjamini-Hochberg corrected p-values (we.eBH) from Welch's t-test are provided, with ASVs included in the table if we.eBH < 0.1. ASV abundance is expressed as the median center log ratio in the combined groups (rab.all). Source indicates the origin of the ASV in the experimental materials (See "ASV tracing to sources "). Taxonomic assignment was performed in Dada2 by reference to the Silva database (v138.1)

ASV	Source	Order	Species	rab.all	Effect	we.eBH
asv0005	*Stigeoclonium* stock	Burkholderiales	*Acidovorax delafieldii*	13,43	−3,41	0,06
asv0002	*Stigeoclonium* stock	Flavobacteriales	*Chryseobacterium* sp.	13,06	−5,53	0,03
asv0021	*Stigeoclonium* stock	Burkholderiales	*Hydrogenophaga palleronii*	11,45	−3,04	0,09
asv0010	*Oedogonium* stock	Sphingomonadales	*Sphingomonas melonis*	11,01	−6	0,03
asv0064	effluent	Chitinophagales	*Edaphobaculum* sp.	9,1	−3,21	0,07
asv0117	unknown	Cytophagales	*Persicitalea* sp.	8,67	−7,51	0,05
asv0133	effluent	Flavobacteriales	*Flavobacterium* sp.	7,95	−5,5	0,03
asv0149	effluent	Sphingomonadales	*Sphingobium* sp.	7,77	−5,43	0,08
asv0116	*Stigeoclonium* stock	Rhizobiales	*Devosia sp.*	7,67	−5	0,09

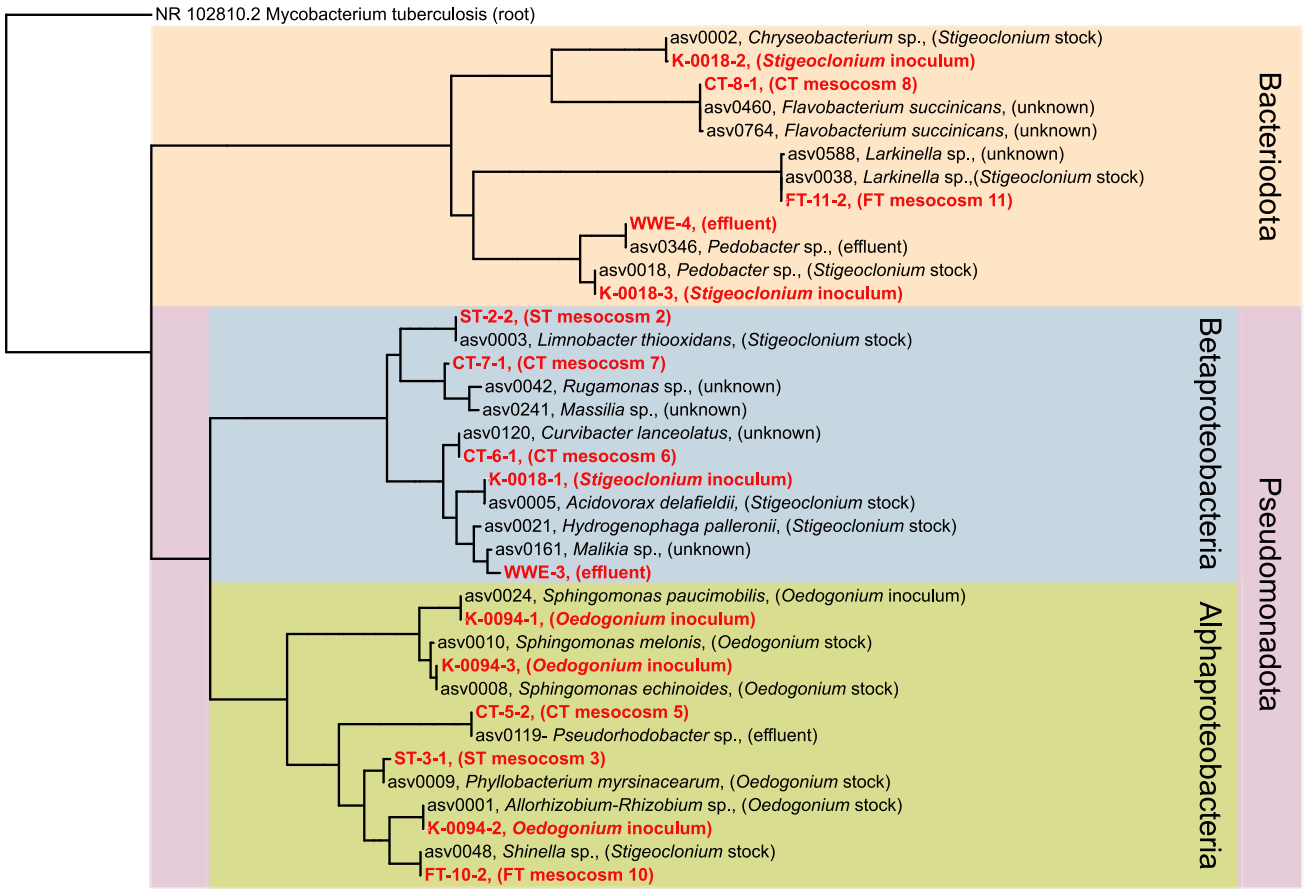


Fig. 8 Maximum likelihood phylogenetic tree pruned to display unique 16S rRNA phylotypes and closely aligned metabarcoding ASVs. The complete unpruned tree can be viewed in the supplemental figure S1. Each phylotype is represented by a single isolated bacterial strain sequence and the isolation environment is indicated in parenthesis. Each ASV sequence includes information about its taxonomic assignment from Dada2 and source is indicated in parenthesis

distinct phylogenetic clades of isolated bacteria (Fig. 8). Bacteria associated with the *Stigeoclonium* inoculum, either based on isolation environment or source tracing of the corresponding ASV, were represented in all three clades while isolates associated with the *Oedogonium* inoculum did not include the phylum Bacteriodota.

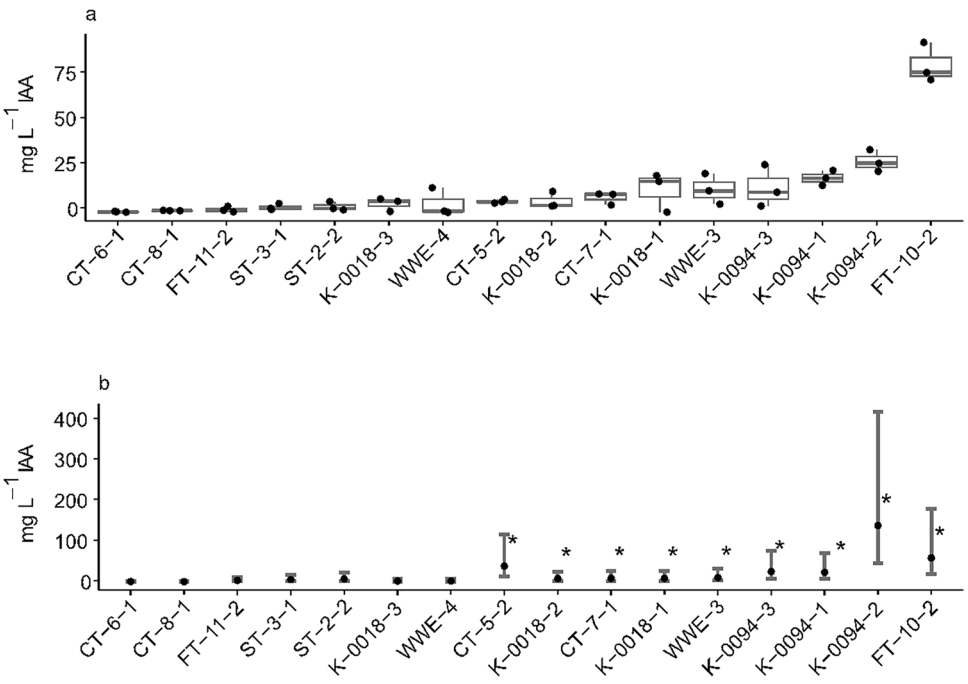


Fig. 9 Screening for IAA content in bacterial strains by the Salkowski method. Measurements were performed on three biological replicate cultures. (**a**) Absorbance at 536 nm is shown as points converted to mg L^{-1} IAA by a standard curve, with box plots illustrating the interquartile range. (**b**) Estimated IAA production, linear model with log(A_{536}/A_{600}) as response and strain as predictor. Predictions of this model can be interpreted as the logarithm of IAA absorbance (560 nm) at unit turbidity (A_{600} = 1) for each strain, 1.96 ×SE as the approximate 95 % CI, an asterisk (*) indicates confidence intervals excluding zero

Auxin screening

Production of the auxin IAA was indicated for several isolated bacterial strains by the Salkowski method. Strain FT-10-2 followed by strain K-0094-2 had the greatest measured IAA in the culture supernatant (Fig. 9a). The estimated production of these two strains was significantly similar when normalized for cell density (Fig. 9b). Observation during culturing suggested that FT-10-2 grows more quickly and to greater density than K-0094-2. Positive results were also observed for strains isolated from the effluent including WWE-3, CT-7-1 and CT-5-2 suggesting that IAA production may be a common bacterial trait in the effluent as well as the algal cultures.

Discussion

Algal growth and phycoremediation potential

The batch cultivation experiment effectively simulated a phycoremediation process, successfully removing residual inorganic nitrogen from the wastewater effluent while accumulating algal biomass. A reduction of inorganic nitrogen from nearly 10 mg L^{-1} to under the lower limits of detection was obtained here, similar to findings from other studies that employed filamentous green algae in phycoremediation (Liu et al. 2020b). For instance, an *Oedogonium* system remediating piggery wastewater reduced ammonium from an initial concentration of 59.4 mg N L^{-1} by more than 95% (Wang et al. 2013). Another relevant study using *Spirogyra* in the remediation of secondary municipal wastewater reduced initial N concentrations from around 10 mg N L^{-1} by more than 99% (Ge et al. 2018).

The present study demonstrates that the VEAS tertiary effluent is suitable for growth of the *Oedogonium* – *Stigeoclonium* co-culture in a batch system. However, nutrient concentrations may require adjustment for continuous operation. The effluent was low in orthophosphate and algal growth was likely supported by luxury uptake during inoculum cultivation. The accumulation and storage of excess phosphorus is well-documented in algae generally and in filamentous chlorophyte algae specifically (Rosemarin 1982, 1983; Lane et al. 2014). Biomass continued to increase until the end of the experiment despite nutrient depletion by day five. Balancing cultivation periods to allow for biomass accumulation while maximizing water remediation and minimizing hydraulic retention time presents potential challenges in the application of this phycoremediation system.

Growth in the ST treatment, where the effluent microbiome had been excluded, was reduced compared to the FT treatment. This was accompanied by a bacterial bloom with the free-living fraction notably dominated by a single ASV (asv0003). This observation is supported by increased bacterial abundance, a low Shannon index and a high Simpson's index. The taxonomic assignment of asv0003 to *Limnobacter thiooxidans* was supported by the isolation of bacterial strains with corresponding sequences. *Limnobacter thiooxidans* is a motile, gram-negative rod shaped bacterium capable of oxidizing thiosulfate and tolerating a wide range of pH and temperatures (Spring et al. 2001).

The greater biomass productivity in the FT treatment is encouraging considering that sterile operation of a phycoremediation system is not practically possible (Renuka et al. 2015; Priyadharshini et al. 2021). It is difficult to infer why sterile filtration of the effluent for the ST treatment resulted in higher bacterial abundance and lower algal productivity or whether these observations are causally linked. However, a potential biological factor not captured by 16S metabarcoding, would be grazing by heterotrophs. Heterotrophic nanoflagellates may have controlled bacteria in the FT treatment if they were not removed by initial filtration steps (Jürgens et al. 1997; Jeuck and Arndt 2013), as they are significant consumers of bacteria in aquatic systems including in wastewater treatment (Martín-Cereceda et al. 2001; Jeuck and Arndt 2013).

Source bacterial communities

To our knowledge, this is the first study using 16S metabarcoding to characterize the bacterial communities of *Oedogonium* and *Stigeoclonium* mono-algal laboratory cultures. The phycosphere communities of these two algal cultures were comprised of bacteria from different taxa. The *Oedogonium* phycosphere was dominated by Alphaproteobacteria Sphingomonas and Rhizobiales while the *Stigeoclonium* phycosphere had a more diverse composition of Pseudomonads and Bacteriodota.

Several studies investigating the assembly of phycospheres have shown significant effects of host selection as well as culture media and stochastic events during culture isolation and maintenance (Kimbrel et al. 2019; Steinrücken et al. 2023; Roager et al. 2024). Host selection of phycosphere communities may be driven in part by differences in the algal exudates produced by the host alga (Seymour et al. 2017; Fu et al. 2020; Blifernez-Klassen et al. 2021; Roager et al. 2024). For example, biotin auxotrophic mutualistic bacteria were selected for within the phycosphere of colonial chlorophyte algae *Botrycoccus*. This highlights that algal exudates including vitamins shape phycosphere bacteria and is evidence of co-evolved autotrophies. It is likely that co-evolved interactions and metabolic dependencies are involved in in maintaining stable phycospheres in microbially rich environments as observed in the present experiments.

Studies of laboratory algal culture phycosphere communities are generally conducted on a limited number of algal strains, either investigating bacterial communities of non-axenic algal cultures (Kimbrel et al. 2019) or laboratory experiments involving the recruitment of phycospheres to axenic cultures from bacterial communities (Fu et al. 2020; Roager et al. 2024). Phycosphere community dynamics and function is further complicated as functional traits in bacteria are not well phylogenetically conserved and the effect on algal hosts may vary within bacterial species (Baker et al. 2022). Wider sequencing efforts and experiments involving a greater diversity of algal hosts are needed to elucidate patterns in phycosphere bacterial diversity and function that can be generalized and applied to algal biotechnology.

The bacterial community of the wastewater effluent was notably more diverse and rich than that of the mono-algal cultures, reflecting the microbial complexity of the wastewater treatment process involving sewage, groundwater, and activated sludge (Wasteson et al. 2020; Vestfjorden Wastewater Company 2023). The effluent community was predominantly composed of Burkholderiales, particularly the genus *Polaromonas*, which is adapted to cold environments and common at high-latitudes (Darcy et al. 2011). However, *Polaromonas* did not sustain its dominance in the CT treatment, demonstrating that the mesocosm culture conditions had a substantial impact on the effluent bacterial community.

Mesocosm bacterial communities

In the algal-inoculated mesocosm treatments (FT and ST), the attached and free-living fractions provide insight into the assembly of bacterial communities in distinct micro-niches and the tendency of algal hosts to select specific community compositions within the phycosphere. The similarity of the attached fractions across treatments indicates that the phycosphere community was able to maintain stability in the microbially rich effluent. This suggests that potential MGPB are capable of sustaining their abundance and competing with environmental bacteria, which is important for practical applications in algal biotechnology (Priyadharshini et al. 2021). Potential MGPB that are able to maintain high abundance during phycoremediation were identified by differential abundance analysis between the attached and free-living fractions of the FT treatment.

Differential abundance analysis revealed that highly abundant ASVs, such as *Chryseobacterium* (asv0002) and *Acidovorax* (asv0005), were more prevalent in the attached community. This suggests that these bacteria are able to maintain a proximal association with the algal biomass. This association with the phycosphere may indicate co-evolved algae – bacteria interactions. While we are able to identify several significantly differentially abundant ASVs, we also consider that many bacteria similarly abundant in the attached and free-living fraction also may have functional roles in the phycosphere. For example, asv0001 was not indicated as significantly differentially abundant, but being one of the most abundant ASVs in both fractions may still indicate association with the phycosphere. This is further supported by tracing asv0001 to the *Oedogonium* stock culture and its phylogenetic assignment to Rhizobiales.

Indication of phytohormones

Phytohormone indole-3-acetic acid (IAA) functions as a key regulator of a wide range of traits in higher plants and algae and is produced by various microorganisms, including bacteria and fungi, many of which engage in symbiotic relationships with algae and plants (De-Bashan et al. 2008; Stirk et al. 2013; Defez et al. 2017; Etesami and Glick 2024). While IAA synthesis and sensitivity to exogenous IAA has been documented in diverse algae, it remains relatively less understood compared to in higher plants (Tarakhovskaya et al. 2007; Stirk et al. 2013). A recent study involving the alga *Chlamydomonas reinhardtii* described a mechanism of algae–bacteria mutualism, in which algal synthesis of the L-tryptophan derivative L-amino acid oxidase (LAO1) leads to increased bacterial IAA production (Calatrava et al. 2024). This suggests that *Chlamydomonas* may play an interkingdom role in regulating exogenous IAA in soils and aquatic systems.

In the present study indole-3-acetic acid (IAA) production was indicated for several isolated bacteria suggesting a mechanism of bacteria–algae interaction. Strain FT-10-2, Rhizobiales, *Shinella* (asv0048), had the highest estimated IAA production. The source of asv0048 was traced to the *Stigeoclonium* stock culture. Another isolated Rhizobiales strain, *Rhizobium* (K-0094-2), also demonstrated potential IAA production and corresponded to the highly abundant asv0001, traced to the *Oedogonium* stock culture. These results indicate that IAA-producing Rhizobiales bacteria may play a role in the phycosphere of both mono-algal inoculum cultures an inference supported by other studies on the functional roles of Rhizobiales in phycospheres (Kim et al. 2014).

In addition to Rhizobiales bacteria, two *Sphingomonas* strains, K-0094-1 (*S. paucimobilis*, asv0024) and K-0094-3 (*S. echinoides*, asv0008), also showed significant indications of IAA production. Both strains were isolated from the *Oedogonium* inoculum and were detected during the experiment. These findings align with literature documenting IAA production and plant growth-promoting traits in both Rhizobiales (Defez et al. 2017; Wang et al. 2020; Cavite et al. 2021) and Sphingomonadales (White et al. 1996; Sukweenadhi et al. 2015). This contributes to the growing evidence of these taxa functioning as MGPB (Kim et al. 2014; Ramanan et al. 2015; Na et al. 2021). Rhizobiales and Sphingomonadales are Alphaproteobacteria and clustered as adjacent clades during phylogenetic analysis of the bacterial isolates (Fig. S1). Further investigation into the roles of Rhizobiales and Sphingomonadales in algal cultures, as well as more refined analyses of phytohormone production in the phycosphere, is warranted.

Conclusion

This laboratory mesocosm experiment reveals valuable insights into the taxonomic composition and role of bacterial communities during phycoremediation. The phycosphere maintained a stable taxonomic composition and community structure during the phycoremediation process. The removal of the wastewater microbiome resulted in reduced algal growth and increased bacterial abundance. These results are encouraging for the algal biotechnology industry where industrial cultivation is subject to non-sterile conditions and may employ microbially rich wastewater as growth media during cultivation.

Several highly abundant potential MGPB from the experiment were isolated and were indicated as auxin IAA producers. The strongest evidence for IAA synthesis was found in isolates from the orders Rhizobiales and Sphingomonadales which is congruent with literature supporting functional roles of these bacterial taxa in phycospheres across a diversity of algal hosts (Kim et al. 2014; Ramanan et al. 2015; Seymour et al. 2017; Na et al. 2021).

Future research should investigate the degree of host specificity and host selection in the assembly of phycosphere communities, and more detailed analyses of phytohormone production by phycosphere-associated bacteria. This can elucidate the mechanisms behind phycosphere bacterial community assembly and the impact on algal growth and phycoremediation efficacy.

Supplementary information The online version contains supplementary material available at https://doi.org/10.1007/s10811-025-03455-7.

Acknowledgements Wastewater effluent for the experiment was provided by VEAS AS treatment plant in Slemmestad, Norway. We thank the Norwegian Water Research Institute (NIVA) staff, Tommy Marelius for his technical support in the construction of the mesocosms as well as sampling during the experiment. As well as Aina Charlotte Wennberg for her support with Flow Cytometry, and Dr. Ana Margarida Costa for her advice and support. Additionally, we are grateful for the support of the University of Oslo Department of Biosciences (IBV) staff for technical support and advice, in particular Dr. Minh Vu for support in the molecular laboratory, as well as Prof. Tom Andersen and Prof. Alexander Eiler for sharing their expert advice.

Author contribution E.W performed the data analysis and wrote the main manuscript as well as prepared all figures and tables. E.W, B.S, K.S, and L.S contributed to the conceptional design of experiments and reviewed the data analyses and the main manuscript.

Funding Open access funding provided by Norwegian Institute For Water Research. This research was supported by the Research Council of Norway through the ALGECO project (project no. 320079).

Data availability Sequence data of bacteria isolates that support this study have been deposited to the National Center for Biotechnology Information (NCBI) GenBank database under code SUB14877682. Metabarcode (eDNA) sequence data has been deposited to the NCBI Sequence Read Archive (SRA) under code PRJNA1190337

Declarations

Conflicts of interest The authors declare that there are no conflicts of interest in regard to this study.

Open Access This article is licensed under a Creative Commons Attribution 4.0 International License, which permits use, sharing, adaptation, distribution and reproduction in any medium or format, as long as you give appropriate credit to the original author(s) and the source, provide a link to the Creative Commons licence, and indicate if changes were made. The images or other third party material in this article are included in the article's Creative Commons licence, unless indicated otherwise in a credit line to the material. If material is not included in the article's Creative Commons licence and your intended use is not permitted by statutory regulation or exceeds the permitted use, you will need to obtain permission directly from the copyright holder. To view a copy of this licence, visit http://creativecommons.org/licenses/by/4.0/.

References

Abellan-Schneyder I, Matchado MS, Reitmeier S, Sommer A, Sewald Z, Baumbach J, List M, Neuhaus K (2021) Primer, pipelines, parameters: issues in 16S rRNA gene sequencing. mSphere 6:e01202-20

Ashraf N, Ahmad F, Lu Y (2023) Synergy between microalgae and microbiome in polluted waters. Trends Microbiol 31:9–21

Baker D, Lauer J, Ortega A, Jackrel SL, Denef VJ (2022) Effects of phycosphere bacteria on their algal host are host species-specific and not phylogenetically conserved. Microorganisms 11:62

Benchling [Biology Software] (2024) Retrieved from https://benchling.com

Blifernez-Klassen O, Klassen V, Wibberg D, Cebeci E, Henke C, Rückert C, Chaudhari S, Rupp O, Blom J, Winkler A (2021) Phytoplankton consortia as a blueprint for mutually beneficial eukaryote-bacteria ecosystems based on the biocoenosis of *Botryococcus* consortia. Sci Rep 11:1726

Blifernez-Klassen O, Hassa J, Reinecke DL, Busche T, Klassen V, Kruse O (2023) Microbial diversity and community structure of wastewater-driven microalgal biofilms. Microorganisms 11:2994

Burgunter-Delamare B, Shetty P, Vuong T, Mittag M (2024) Exchange or eliminate: The secrets of algal-bacterial relationships. Plants 13:829

Calatrava V, Hom EFY, Guan Q, Llamas A, Fernández E, Galván A (2024) Genetic evidence for algal auxin production in *Chlamydomonas* and its role in algal-bacterial mutualism. iScience 27:108762

Callahan BJ, McMurdie PJ, Rosen MJ, Han AW, Johnson AJA, Holmes SP (2016) DADA2: High-resolution sample inference from Illumina amplicon data. Nat Methods 13:581–583

Cavite HJM, Mactal AG, Evangelista EV, Cruz JA (2021) Growth and yield response of upland rice to application of plant growth-promoting rhizobacteria. J Plant Growth Regul 40:494–508

Darcy JL, Lynch RC, King AJ, Robeson MS, Schmidt SK (2011) Global distribution of *Polaromonas* phylotypes-evidence for a highly successful dispersal capacity. PLoS One 6:e23742

Davis NM, Proctor DM, Holmes SP, Relman DA, Callahan BJ (2018) Simple statistical identification and removal of contaminant sequences in marker-gene and metagenomics data. Microbiome 6:226

De-Bashan LE, Antoun H, Bashan Y (2008) Involvement of indole-3-acetic acid produced by the growth-promoting bacterium *Azospirillum* spp. in promoting growth of *Chlorella vulgaris*. J Phycol 44:938–947

Defez R, Andreozzi A, Dickinson M, Charlton A, Tadini L, Pesaresi P, Bianco C (2017) Improved drought stress response in alfalfa plants nodulated by an IAA over-producing *Rhizobium* strain. Front Microbiol 8:2466

Durán P, Flores-Uribe J, Wippel K, Zhang P, Guan R, Melkonian B, Melkonian M, Garrido-Oter R (2022) Shared features and reciprocal complementation of the *Chlamydomonas* and *Arabidopsis* microbiota. Nat Commun 13:406

Etesami H, Glick BR (2024) Bacterial indole-3-acetic acid: A key regulator for plant growth, plant-microbe interactions, and agricultural adaptive resilience. Microbiol Res 281:127602

Fu H, Uchimiya M, Gore J, Moran MA (2020) Ecological drivers of bacterial community assembly in synthetic phycospheres. Proc Natl Acad Sci USA 117:3656–3662

Fulbright SP, Robbins-Pianka A, Berg-Lyons D, Knight R, Reardon KF, Chisholm ST (2018) Bacterial community changes in an industrial algae production system. Algal Res 31:147–156

Gang S, Sharma S, Saraf M, Buck M, Schumacher J (2019) Analysis of indole-3-acetic acid (IAA) production in *Klebsiella* by LC-MS/MS and the Salkowski method. Bio Protoc 9:e3230

Ge S, Madill M, Champagne P (2018) Use of freshwater macroalgae *Spirogyra* sp. for the treatment of municipal wastewaters and biomass production for biofuel applications. Biomass Bioenergy 111:213–223

Glick BR (2012) Plant growth-promoting bacteria: mechanisms and applications. Scientifica 2012:963401

Gloor G (2015) ALDEx2: ANOVA-Like Differential Expression tool for compositional data. ALDEX Man Modular 20:1–11

Illumina (2013) 16S metagenomic sequencing library preparation preparing 16S ribosomal RNA Gene amplicons for the Illumina MiSeq system. San Diego. https://www.illumina.com/content/dam/illumina-support/documents/documentation/chemistry_documentation/16s/16s-metagenomic-library-prep-guide-15044223-b.pdf

Jeuck A, Arndt H (2013) A short guide to common heterotrophic flagellates of freshwater habitats based on the morphology of living organisms. Protist 164:842–860

Jürgens K, Arndt H, Zimmermann H (1997) Impact of metazoan and protozoan grazers on bacterial biomass distribution in microcosm experiments. Aquat Microb Ecol 12:131–138

Källqvist T, Molvær J, Oug E, Berge D, Tjomsland T, Stene-Johansen S (2002) Implementation of the urban waste water treatment directive in Norway-An evaluation of the Norwegian approach regarding wastewater treatment. Norwegian Institute for Water Research Report 4466-2001, p 70

Kim B-H, Ramanan R, Cho D-H, Oh H-M, Kim H-S (2014) Role of *Rhizobium*, a plant growth promoting bacterium, in enhancing algal biomass through mutualistic interaction. Biomass Bioenergy 69:95–105

Kimbrel JA, Samo TJ, Ward C, Nilson D, Thelen MP, Siccardi A, Zimba P, Lane TW, Mayali X (2019) Host selection and stochastic effects influence bacterial community assembly on the microalgal phycosphere. Algal Res 40:101489

Lane DJ, Zevenhoven M, Ashman PJ, van Eyk PJ, Hupa M, de Nys R, Lewis DM (2014) Algal biomass: occurrence of the main inorganic elements and simulation of ash interactions with bed material. Energy Fuels 28:4622–4632

Liu B, Eltanahy EE, Liu H, Chua ET, Thomas-Hall SR, Wass TJ, Pan K, Schenk PM (2020a) Growth-promoting bacteria double eicosapentaenoic acid yield in microalgae. Bioresour Technol 316:123916

Liu J, Pemberton B, Lewis J, Scales PJ, Martin GJ (2020b) Wastewater treatment using filamentous algae–a review. Bioresour Technol 298:122556
Martin M (2011) Cutadapt removes adapter sequences from high-throughput sequencing reads. J Environ Public Health 17:10–12
Martín-Cereceda M, Pérez-Uz B, Serrano S, Guinea A (2001) Dynamics of protozoan and metazoan communities in a full scale wastewater treatment plant by rotating biological contactors. Microbiol Res 156:225–238
McLaren M (2020) speedyseq: Faster implementations of common phyloseq functions. https://github.com/mikemc/speedyseq
McMurdie PJ, Holmes S (2013) phyloseq: an R package for reproducible interactive analysis and graphics of microbiome census data. PLOS One 8:e61217
Na H, Jo SW, Do JM, Kim IS, Yoon HS (2021) Production of algal biomass and high-value compounds mediated by interaction of microalgal *Oocystis* sp. KNUA044 and bacterium *Sphingomonas* KNU100. J Microbiol Biotechnol 31:387–397
Nearing JT, Douglas GM, Hayes MG, MacDonald J, Desai DK, Allward N, Jones CM, Wright RJ, Dhanani AS, Comeau AM (2022) Microbiome differential abundance methods produce different results across 38 datasets. Nat Commun 13:342
Palacios OA, López BR, de Bashan LE (2022) Microalga Growth-Promoting Bacteria (MGPB): A formal term proposed for beneficial bacteria involved in microalgal–bacterial interactions. Algal Res 61:102585
Prest E, Hammes F, Kötzsch S, van Loosdrecht MC, Vrouwenvelder JS (2013) Monitoring microbiological changes in drinking water systems using a fast and reproducible flow cytometric method. Water Res 47:7131–7142
Priyadharshini SD, Babu PS, Manikandan S, Subbaiya R, Govarthanan M, Karmegam N (2021) Phycoremediation of wastewater for pollutant removal: a green approach to environmental protection and long-term remediation. Environ Pollut 290:117989
Ramanan R, Kang Z, Kim B-H, Cho D-H, Jin L, Oh H-M, Kim H-S (2015) Phycosphere bacterial diversity in green algae reveals an apparent similarity across habitats. Algal Res 8:140–144
Reasoner DJ, Geldreich E (1985) A new medium for the enumeration and subculture of bacteria from potable water. Appl Environ Microbiol 49:1–7
Renuka N, Sood A, Prasanna R, Ahluwalia A (2015) Phycoremediation of wastewaters: a synergistic approach using microalgae for bioremediation and biomass generation. Int J Environ Sci Technol 12:1443–1460
Roager L, Kempen PJ, Bentzon-Tilia M, Sonnenschein EC, Gram L (2024) Impact of host species on assembly, composition, and functional profiles of phycosphere microbiomes. mSystems 9:e00583-00524
Rosemarin AS (1982) Phosphorus nutrition of two potentially competing filamentous algae, *Cladophora glomerata* (L.) Kütz. and *Stigeoclonium tenue* (Agardh) Kütz. from Lake Ontario. J Great Lakes Res 8:66–72
Rosemarin AS (1983) Direct examination of growing filaments to determine phosphate growth kinetics in *Cladophora glomerata* (L.) Kütz and *Stigeoclonium tenue* (Agardh) Kütz. In: Wetzel RG (ed) Periphyton of Freshwater Ecosystems: Proceedings of the First International Workshop on Periphyton of Freshwater Ecosystems held in Växjö, Sweden. Dr W Junk, The Hague, pp 111–119
Schliep KP (2019) Estimating phylogenetic trees with phangorn
Seymour JR, Amin SA, Raina J-B, Stocker R (2017) Zooming in on the phycosphere: the ecological interface for phytoplankton–bacteria relationships. Nat Microbiol 2:1–12
Spring S, Kämpfer P, Schleifer KH (2001) *Limnobacter thiooxidans* gen. nov., sp. nov., a novel thiosulfate-oxidizing bacterium isolated from freshwater lake sediment. Int J Syst Evol Microbiol 51:1463–1470
Steinrücken P, Jackson S, Müller O, Puntervoll P, Kleinegris DM (2023) A closer look into the microbiome of microalgal cultures. Front Microbiol 14:1108018
Stirk WA, Ördög V, Novák O, Rolčík J, Strnad M, Bálint P, van Staden J (2013) Auxin and cytokinin relationships in 24 microalgal strains. J Phycol 49:459–467
Sukweenadhi J, Kim Y-J, Kang CH, Farh ME-A, Nguyen N-L, Hoang V-A, Choi E-S, Yang D-C (2015) *Sphingomonas panaciterrae* sp. nov., a plant growth-promoting bacterium isolated from soil of a ginseng field. Arch Microbiol 197:973–981
Tarakhovskaya E, Maslov YI, Shishova M (2007) Phytohormones in algae. Russ J Plant Physiol 54:163–170
Van Den Hendeb S (2015) SOP: 2.5. b Analysis of dissolved orthophosphate using a colorimetric method. In: Silikana A, Flynn KJ, Llewellyn CA, Bayliss C (eds) Standard operating procedures for analytical methods and data collection in support of pilot-scale cultivation of microalgae. EnAlgae Report WP1A3.01, pp 137–141
Vestfjorden Wastewater Company (2023) From sewage treatment plant to biorefinery. Retrieved September 2024, from website https://veas.nu/arsrapporter
Wang H, Hu Z, Xiao B, Cheng Q, Li F (2013) Ammonium nitrogen removal in batch cultures treating digested piggery wastewater with microalgae *Oedogonium* sp. Water Sci Technol 68:269–275
Wang S, Meade A, Lam H-M, Luo H (2020) Evolutionary timeline and genomic plasticity underlying the lifestyle diversity in Rhizobiales. Systems 5:e00438-20
Wasteson Y, Blix HS, Joner E, Madslien EH, Ottoson J, Sørum H, Uhl W, Yazdankhah SP, Bergh Ø, Eklo OM (2020) Assessment of the impact of wastewater and sewage sludge treatment methods on antimicrobial resistance. In: scientific opinion of the panel on microbial ecology of the Norwegian scientific committee for food and environment. Scientific opinion of the Panel on Microbial Ecology of the Norwegian Scientific Committee for Food and Environment. VKM Report 2020:08
Watanabe M (2005) Freshwater culture media. In: Andersen RA (ed) Algal culturing techniques. Elsevier, Burlington, pp 13–20
White DC, Sutton SD, Ringelberg DB (1996) The genus *Sphingomonas*: physiology and ecology. Curr Opin Biotechnol 7:301–306
Willis A, Bunge J (2015) Estimating diversity via frequency ratios. Biometrics 71:1042–1049
Willis AD, Martin BD (2022) Estimating diversity in networked ecological communities. Biostatistics 23:207–222

Publisher's note Springer Nature remains neutral with regard to jurisdictional claims in published maps and institutional affiliations.